



Wdr63 Deletion Aggravates Ulcerative Colitis Likely by Affecting Th17/Treg Balance and Gut Microbiota*

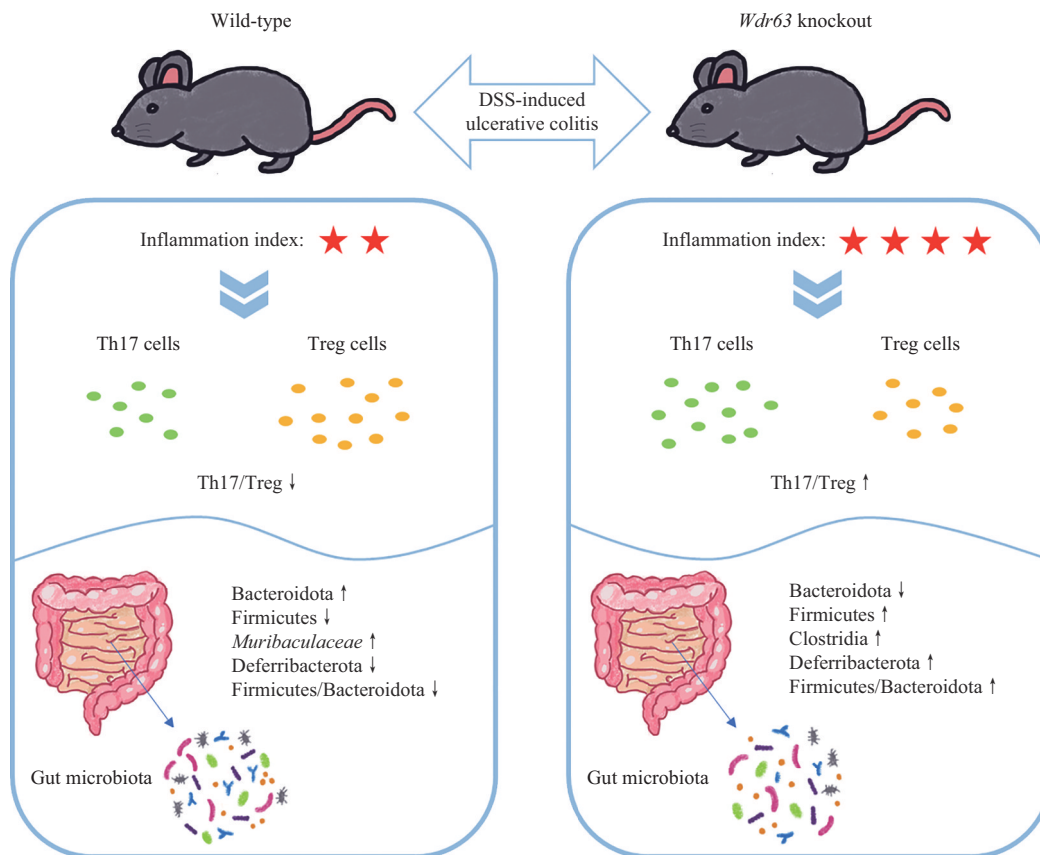
ZHU Hao¹⁾, ZHU Meng-Yuan¹⁾, CAO Yang-Yang¹⁾, YANG Qiu-Bo^{1)**}, FAN Zhi-Peng^{1,2,3)**}

¹⁾Beijing Institute for Dental Research, Capital Medical University School of Stomatology, Beijing 100050, China;

²⁾Beijing Laboratory of Oral Health, Capital Medical University, Beijing 100069, China;

³⁾Research Unit of Tooth Development and Regeneration, Chinese Academy of Medical Sciences, Beijing 100069, China)

Graphical abstract



* This work was supported by grants from The National Natural Science Foundation of China (82130028), National Key Research and Development Program (2022YFA1104401), CAMS Innovation Fund for Medical Sciences (2019-I2M-5-031), and Innovation Research Team Project of Beijing Stomatological Hospital, Capital Medical University (CXTD202204).

** Corresponding author.

FAN Zhi-Peng. Tel: 86-10-57099311, E-mail: zpfan@ccmu.edu.cn

YANG Qiu-Bo. Tel: 86-10-57099319, E-mail: qiuboyang2003@163.com

Received: April 8, 2024 Accepted: August 21, 2024

Abstract Objective Ulcerative colitis is a prevalent immunoinflammatory disease. Th17/Treg cell imbalance and gut microbiota dysregulation are key factors in ulcerative colitis pathogenesis. The actin cytoskeleton contributes to regulating the proliferation, differentiation, and migration of Th17 and Treg cells. *Wdr63*, a gene containing the WD repeat domain, participates in the structure and functional modulation of actin cytoskeleton. Recent research indicates that WDR63 may serve as a regulator of cell migration and metastasis *via* actin polymerization inhibition. This article aims to explore the effect of *Wdr63* deletion on Th17/Treg cells and ulcerative colitis. **Methods** We constructed *Wdr63*^{-/-} mice, induced colitis in mice using dextran sulfate sodium salt, collected colon tissue for histopathological staining, collected mesenteric lymph nodes for flow cytometry analysis, and collected healthy mouse feces for microbial diversity detection. **Results** Compared with wild-type colitis mice, *Wdr63*^{-/-} colitis mice had a more pronounced shortening of colonic tissue, higher scores on disease activity index and histological damage index, Treg cells decreased and Th17 cells increased in colonic tissue and mesenteric lymph nodes, a lower level of anti-inflammatory cytokine IL-10, and a higher level of pro-inflammatory cytokine IL-17A. In addition, WDR63 has shown positive effects on maintaining intestinal microbiota homeostasis. It maintains the balance of Bacteroidota and Firmicutes, promoting the formation of beneficial intestinal bacteria linked to immune inflammation. **Conclusion** *Wdr63* deletion aggravates ulcerative colitis in mice, WDR63 inhibits colonic inflammation likely by regulating Th17/Treg balance and maintains intestinal microbiota homeostasis.

Key words *Wdr63*, Th17/Treg, ulcerative colitis, inflammation, immune, microbiology

DOI: 10.16476/j.pibb.2024.0148

CSTR: 32369.14.pibb.20240148

Inflammatory bowel disease (IBD) is a relapsing, nonspecific, chronic inflammatory disease, encompassing Crohn's disease and ulcerative colitis (UC) [1]. Patients with IBD commonly experience symptoms such as stomach pain, rectal bleeding, diarrhea, and body mass loss [2]. The global incidence of IBD has been increasing in recent years [3-4]. While the pathology of IBD remains incompletely understood, evidence suggests that abnormal immune responses and dysbiosis of the intestinal microbiota closely correlate with its development [5-6]. In genetically susceptible hosts, IBD seems to arise from overly aggressive immune responses by T cells targeting specific components of the intestinal microbiota, which are triggered and reactivated by environmental factors [7]. Presently, no ideal therapeutic drug for IBD exists that is highly effective and devoid of side effects; traditional treatments merely alleviate symptoms without curing the disease [8-10]. Targeting T cells shows promise in treating intestinal inflammation owing to their pivotal role in the immune response.

As significant activators of the immune system, CD4 T cells play a critical role in regulating human health and disease [11]. CD4 T cells rely on a balance among various T cell subsets to function properly and trigger the host's immune system against threats [12]. Among these, the balance between T helper type 17 (Th17) and regulatory T (Treg) cells is essential to maintain immune homeostasis [13]. Th17 cells promote

self-immunization and inflammation at the site of infection, while Treg cells dampen autoimmunity and control tissue inflammation through immune tolerance [14-15]. Th17/Treg cells imbalance can lead to tissue damage and the development of immune-inflammatory diseases, including IBD [16], periodontitis [17], and rheumatoid arthritis [18]. In IBD, Th17/Treg cells link the gut microbiota to host metabolic dysfunction and promote gut microbiota to alleviate IBD [19]. Various factors, such as cytokine signals, T cell receptor signals, metabolism, and the microbiota, impact the development and upkeep of Th17 and Treg cells, which are essential to regulate the balance between them [20].

The actin cytoskeleton is a critical component of eukaryotic cells, as it contributes to various cellular functions, including regulating cell proliferation, migration, and differentiation [21-22]. The dynamic remodeling of the actin cytoskeleton is vital for T lymphocyte effector function [23]. It is widely accepted that T cell activation, particularly the migration of T cell receptor microclusters during immune synapse formation, depends on cytoskeletal remodeling [24]. The activation of CD4 T cells induces actin polymerization in both the nucleus and cytoplasm, facilitated by the Arp2/3 complex. This, in turn, triggers the expression of cytokines and enhances T cell receptor signaling [25]. Meanwhile, the actin cytoskeleton facilitates the necessary forces and shape changes that drive T-cell migration in complex environments [26]. Notch is a critical regulator of T cell

differentiation, and PKC θ links proximal T cell and Notch signaling through localized regulation of the actin cytoskeleton^[27]. In addition, actin cytoskeleton remodeling is crucial for Treg cell homeostasis and suppressive functions as well^[28].

Wdr63 is a WD repeat structural domain-containing gene associated with actin cytoskeleton formation. It acts in the mesenchymal stem cell (MSC)-mediated tissue regeneration and osteogenic differentiation of odontogenic MSCs^[29]. *Wdr63* intragenic deletion is the likely cause of human occipital encephalocele and abnormal central nervous system development in zebrafish^[30]. As a member of the dynein group, it is also involved in the formation and movement of cilia and flagella, and double allelic variants of WDR63 can cause male infertility^[31-33]. Recent studies have shown that WDR63 functions as a negative regulator of cell migration, invasion, and metastasis by inhibiting actin polymerization mediated by the Arp2/3 complex^[34]. However, the function of WDR63 in T cell proliferation and differentiation is unknown, and its impact on Th17/Treg cell homeostasis remains uncertain.

Our study evaluated *in vivo* the impact of WDR63 on Th17/Treg cell homeostasis and gut microbiology in mice colitis models of dextran sodium sulfate salt (DSS)-induced. The results suggest that *Wdr63* deletion aggravated colitis induced by DSS. WDR63 acted as an anti-inflammatory agent by maintaining Th17/Treg cell homeostasis and regulating microbial community homeostasis. This study provides new insights into immune-mediated inflammatory disease treatment.

1 Materials and methods

1.1 Animals

The study was permitted under the Animal Care and Use Committee of Beijing Stomatological Hospital, affiliated with Capital Medical University (Ethical Review No. KQYY-202205-003). We used animals following the guidelines of the Regulations on the Management of Laboratory Animals. The experimental animals were 6–8 weeks old C57BL/6 mice. *Wdr63* knockout (*Wdr63*^{-/-}) mice were generated based on CRISPR/Cas9 technology. The positive founder (F0-generation) mice (*Wdr63*^{+/-}) were provided by the Biocytogen Pharmaceuticals (Beijing) Co., Ltd, and the heterozygous F1-generation mice were

derived by intercrossing heterozygous F0-generation and wild-type (WT) mice, followed by crossing homozygous F1-generation heterozygote mice to generate animals used in all experiments of this study. Mice were genotyped using Quick Genotyping Assay Kit for Mouse Tail (Cat#: D7283S, Beyotime, China) following the manufacturer's instructions. Both wild-type and knockout mice used in the experiments were raised in the same environment under the same conditions.

1.2 Induction of the UC model

The experimental groups were two groups of WT mice (control group) and *Wdr63*^{-/-} mice (experimental group), with 8 mice in each group, and the experimental UC model was induced by using 3% (*w/v*) DSS (#02160110-CF, MP Biomedicals, USA) solution as drinking water fed to mice for 7 d.

1.3 Disease activity index (DAI) score

During the experimental period, we recorded the body mass and fecal matter of mice at 10 am each day. Scoring of each mouse based on DAI criteria. Scoring criteria was as follows. (1) No mass loss is scored as 0; 1%–5% mass loss is scored as 1; 5%–10% mass loss is scored as 2; 10%–15% mass loss is scored as 3; and more than 15% mass loss is scored as 4. (2) Normal stool texture is scored as 0; loose stool is scored as 2; and diarrhea is scored as 4. (3) Negative fecal occult blood is 0 points; positive fecal occult blood is 2 points; and rectal bleeding is 4 points. The total of three scores above is the DAI score.

1.4 Histologic examination

Colon tissues were collected, fixed in 4% paraformaldehyde, dehydrated, and embedded in paraffin. We then cut the tissue blocks into 5 μ m slices. And the final assessment of inflammation in colonic tissue by hematoxylin and eosin (H&E) staining. Images were captured under a microscope (Olympus, Japan). The extent of colonic injury and inflammatory infiltration was assessed score using the histological injury index. According to Rachmilewitz *et al.*^[35], parameters associated with colonic pathology include neutrophil margination and infiltration in tissue, hemorrhagic congestion and edema of the mucosa, cuprocyte depletion, and crypt loss. The degree of colonic histopathology was determined and scored based on these. With a score of 0 for no colonic change; minimal change is scored as 1; minor

change is scored as 2; moderate change is scored as 3; and severe change is scored as 4. A score of 0 indicates no inflammatory damage to the colon, while higher scores indicate more inflammatory damage.

1.5 Flow cytometry

On the seventh day of DSS induction, we separated mouse mesenteric lymph nodes and then incubated them in PBS buffer solution supplemented with 0.5% BSA. The mice's lymph nodes were thoroughly ground using 70 μm filter and rinsed with buffer solution after each grinding. Total mesenteric lymph node cells were obtained through centrifugation of the tissue suspension (1 500 r/min for 6 min) and discarding the supernatant. We used the FITC anti-mouse CD4 antibody (#100406, BioLegend, USA) and APC anti-mouse FOXP3 antibody (#APC-65089, Proteintech, USA) for Treg cells fluorescence staining. The CD4 antibody and PE anti-mouse IL-17A antibody (#506904, BioLegend, USA) were used for Th17 cells fluorescence staining. Flow cytometry was performed for final analysis.

1.6 Immunohistochemical analysis

The antigen repair of tissue sections was performed in 0.1 mol/L citrate buffer heated to 95°C for 15 min, followed by incubation in endogenous peroxidase blocking buffer for 10 min at room temperature. Then blocked non-specific antibody binding with PBS containing 1% Triton X-100 (#T8200, Solarbio Life Sciences, China) and 5% BSA for 30 min at room temperature to reduce background staining and interfering factors, stained with FOXP3 (1 : 400, #12653S, Cell Signaling Technology, USA) and ROR γ t (1 : 500, #bs-23110R, Bioss, China) primary antibody overnight at 4°C. Then, the tissues were incubated in biotinylated goat anti-rabbit secondary antibody solution for 10 min, followed by another 10 min of incubation in streptavidin-HRP. Lastly, the sample was stained with DAB solution (#CW2069S, Cwbio, China). The same exposure and intensity settings were used for all images. The results were analyzed using Image J software.

1.7 Enzyme-linked immunosorbent assay (ELISA)

Blood samples were taken from mice, and left to stand for 30 min at room temperature. This was followed by centrifugation for 10 min (3 000 r/min at 4°C). The upper layer of serums was collected. The samples were ultimately transferred to a 96-well

ELISA plate. The concentrations of IL-10 and IL-17A were evaluated using Mouse IL-10 Pre-coated ELISA Kit (Cat#: 1211002, Dakewe Biotech Co., Ltd.) and Mouse IL-17A Pre-coated ELISA Kit (Cat#: 1211702, Dakewe Biotech Co., Ltd.) following the manufacturer's instructions.

1.8 DNA extraction and 16S rRNA amplicon sequencing

After collection, the caecal content samples were immediately frozen at -80°C and kept. Bacterial DNA was extracted from the caecal contents utilizing a DNeasy PowerSoil kit (Qiagen, Hilden, Germany) according to the instructions provided by the manufacturer. A NanoDrop 2000 spectrophotometer (Thermo Fisher Scientific, Waltham, MA, USA) and agarose gel electrophoresis were utilized to determine the concentration and integrity of DNA, respectively. In the 25 μl reaction, universal primer pairs (343F: 5'-TACGGRAGGCAGCAG-3'; 798R: 5'-AGGGTATCTAATCCT-3') were utilized to amplify the V3-V4 hypervariable regions of the bacterial 16S rRNA gene. Gel electrophoresis was utilized to assess the amplicon quality. Purified PCR products were measured. For sequencing, the concentrations were changed appropriately. Two paired-end read cycles of 250 bases each were used during the sequencing process on an Illumina NovaSeq 6000 (Illumina Inc., San Diego, CA). Using DADA2 and QIIME 2's default settings, the paired-end reads were filtered for low-quality sequences, denoised, merged, and verified for chimera reads. Finally, the software produced the abundance table of Amplicon Sequence Variants (ASVs) and representative reads. The investigation of alpha and beta diversity used QIIME 2 software. The *t* test/Wilcoxon statistical test was then used to evaluate the significant differences between the various groups using the R package. The abundance spectrum of taxonomy was compared using the linear discriminant analysis effect size (LEfSe) approach.

1.9 Statistical analysis

The data was presented as mean \pm standard error of the mean (SEM). The statistical analyses were conducted using GraphPad Prism version 8.0 software. Significance was examined using either Student's *t* test or Wilcoxon rank sum test, and a *P* value less than 0.05 was deemed statistically significant.

2 Results

2.1 Generation of *Wdr63* knockout mice

We generated the positive founder (F0-generation) mice (*Wdr63*^{+/-}) by applying CRISPR-Cas9 technology (Figure 1a), and the heterozygous

F1-generation mice were derived by intercrossing heterozygous F0-generation and wide-type mice, followed by crossing homozygous F1-generation heterozygote mice to generate mice used in all experiments of this study. Then identified the genotype of the mice by PCR (Figure 1b).

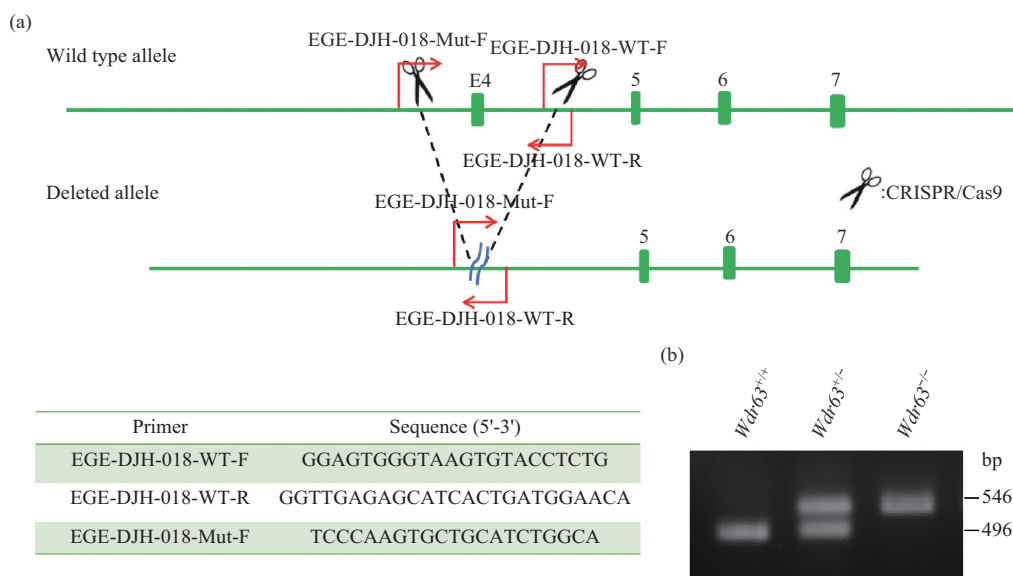


Fig. 1 CRISPR/Cas9 strategy and results for *Wdr63*^{-/-} mouse model

(a) CRISPR/Cas9 strategy map for constructing *Wdr63*^{-/-} mice. Forward (F) and reverse (R) primers are presented for validation and genotyping. (b) Genotype identification of mice by PCR.

2.2 *Wdr63* deletion aggravates dextran sulfate sodium-induced colitis

As Figure 2a shows, the body masses of WT and *Wdr63*^{-/-} mice decreased gradually over time. Among them, the *Wdr63*^{-/-} mice lost more masses. Between-group variation was statistically significant from day 3 to day 7. In addition, *Wdr63*^{-/-} mice exhibited significantly worse colitis symptoms such as loose and bloody stools, and their DAI scores were higher than WT mice, which were statistically significant from day 4 to day 7 (Figure 2b). On the seventh day, each mouse's colon was photographed and measured. The findings indicated that the *Wdr63*^{-/-} mice exhibited a shorter colon length compared to the WT mice (Figure 2c), and the results of quantitative analysis were statistically different (Figure 2d).

H&E staining of colonic tissues showed incomplete colonic tissue with disruption of mucosal continuity and large ulcers in *Wdr63*^{-/-} mice. The glands exhibited a highly irregular shape, with a

decrease in cup cells and extensive infiltration of inflammatory cells into the lamina propria (Figure 2e). In WT mice, colonic mucosal destruction was less severe, the coexistence of damaged and intact mucosa, and inflammatory cells infiltration was reduced. The histological injury index is depicted in Figure 2f for the two groups of mice, with the *Wdr63*^{-/-} mice scoring higher compared to the WT mice. The supplementary figure shows normal colon tissue and H&E staining of colon tissue section in healthy WT and *Wdr63*^{-/-} mice (Figure S1).

2.3 *Wdr63* deletion affects Th17/Treg balance in DSS-induced colitis mice

To investigate the impact of WDR63 on Th17/Treg cell balance, we assessed the proportions of Th17 and Treg cells in the mesenteric lymph nodes. We found the percentage of Th17 cells (CD4⁺ IL-17A⁺) in the mesenteric lymph nodes of *Wdr63*^{-/-} mice was higher compared to WT mice (Figure 3a, b), while the percentage of Treg cells (CD4⁺ Foxp3⁺)

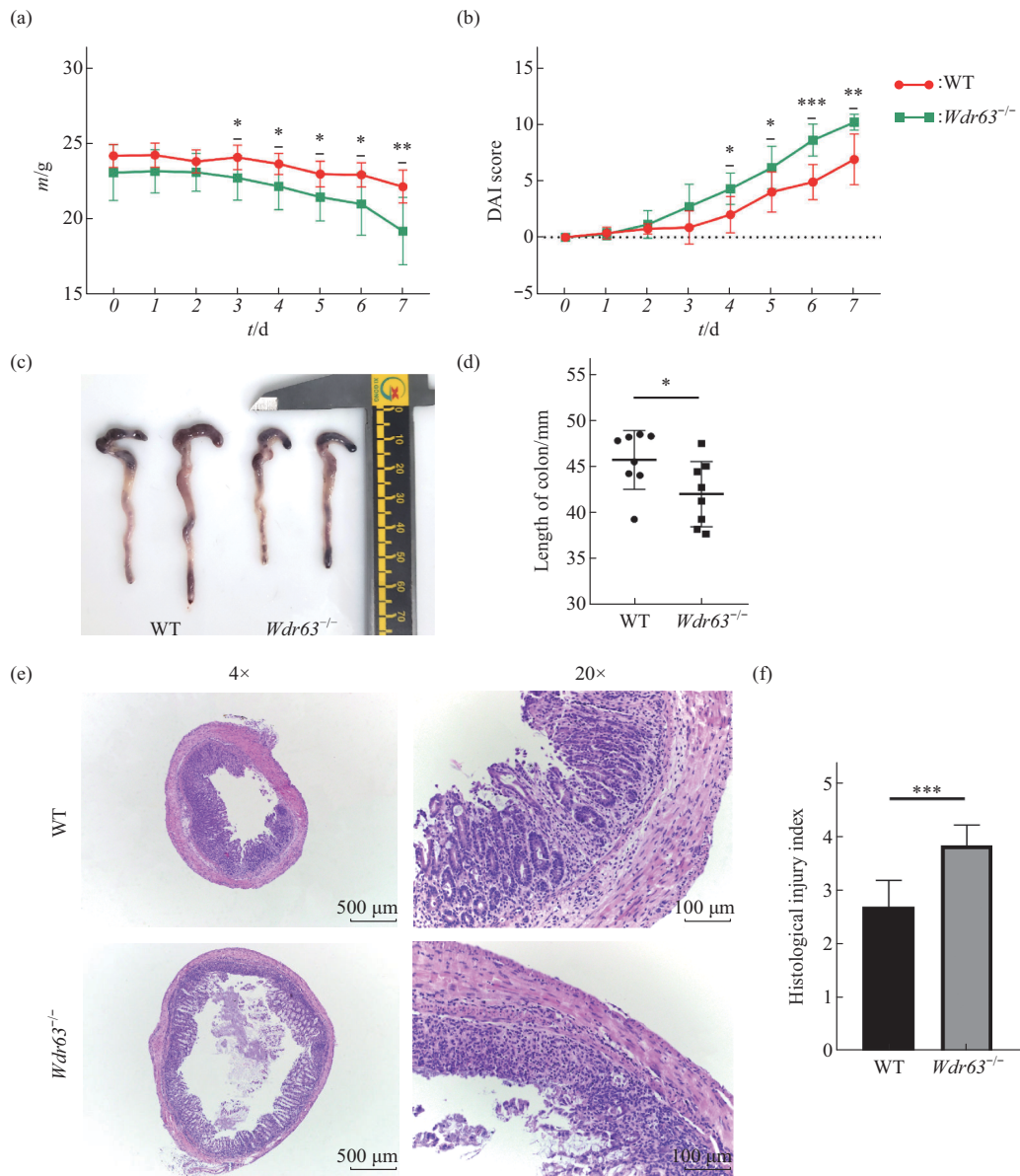


Fig. 2 *Wdr63* deletion aggravates colitis induced by DSS in mice

(a) Body mass of mice at a fixed time of day. (b) DAI scores during the experiment. (c, d) Colon representative pictures (c) in two groups of mice and quantitative assessment of colon length (d). (e) H&E staining of colon sections. (f) Histological injury index. ($n=8$) The statistical indicators were analyzed using two-tailed unpaired t test, with statistical significance being characterized by $P<0.05$. Significant level: * $P<0.05$, ** $P<0.01$, *** $P<0.001$.

was lower (Figure 3c, d). Immunohistochemical staining and quantitative measurements showed the weaker ROR γ t expression in WT mice (Figure 3e, f). However, the *Wdr63*^{-/-} mice had stronger ROR γ t expression in the lamina propria. In contrast, the degree of FOXP3 expression in the colon of the WT mice surpassed that in the *Wdr63*^{-/-} mice (Figure 3g, h). We explored whether WDR63 could regulate the

production of cytokines related to Th17/Treg balance by ELISA. As shown in Figure 3i, j, the expression level of IL-10 was lower in *Wdr63*^{-/-} mice than WT mice, and the expression of IL-17A was significantly increased in *Wdr63*^{-/-} than in WT. In summary, the *Wdr63* deletion reduced the infiltration of protective Treg cells in UC mice colon, while increasing pro-inflammatory Th17 cells.

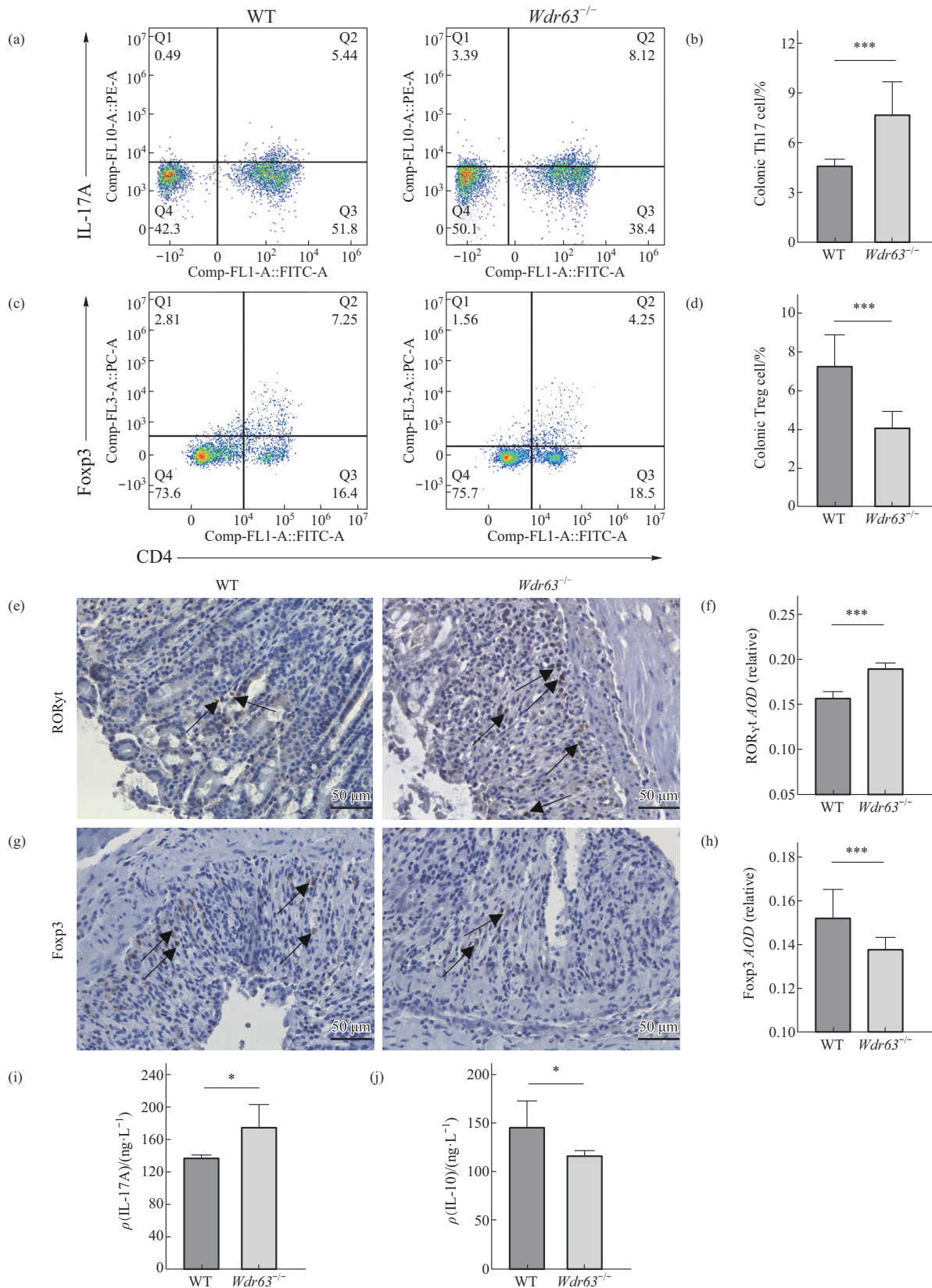


Fig. 3 Effect of *Wdr63* deletion on Th17/Treg cell balance in UC mice

(a) Percentage of the CD4⁺ IL-17A⁺ cell population that are Th17 cells. (b) Statistical analysis of the Th17. (c) Percentage of the CD4⁺ Foxp3⁺ cell population that are Tregs. (d) Statistical analysis of the Tregs. (e–h) The expression of ROR γ t (e) and Foxp3 (g) in colon tissues was detected by immunohistochemistry, and ROR γ t⁺ (f) and Foxp3⁺ (h) cells were quantified. AOD: average optical density. (i, j) Concentrations of IL-17A (i) and IL-10 (j) in the serum of mice in both groups. The statistical indicators were analyzed using two-tailed unpaired *t* test, with statistical significance being characterized by $P < 0.05$. Significant levels: * $P < 0.05$, *** $P < 0.001$.

2.4 *Wdr63* deletion alters the gut microbiota in mice

To explore the possible impact of WDR63 on gut microbiota, we analyzed fecal samples from healthy WT and *Wdr63*^{-/-} mouse *via* high-throughput sequencing of the 16S rRNA. Compared to the WT mice, the α -diversity index showed that Chao1 (Figure 4a) and Shannon index (Figure 4b) were

higher and the Simpson index (Figure 4c) showed lower values in *Wdr63*^{-/-} mice. *Wdr63* deletion affected the abundance and diversity of gut microbiota in mice. The principal coordinate analysis revealed the β -diversity of intestinal flora. The study found the species diversity of the intestinal flora in WT and *Wdr63*^{-/-} mice were separated, and the structure of the intestinal microbial communities in the two groups was different (Figure 4d).

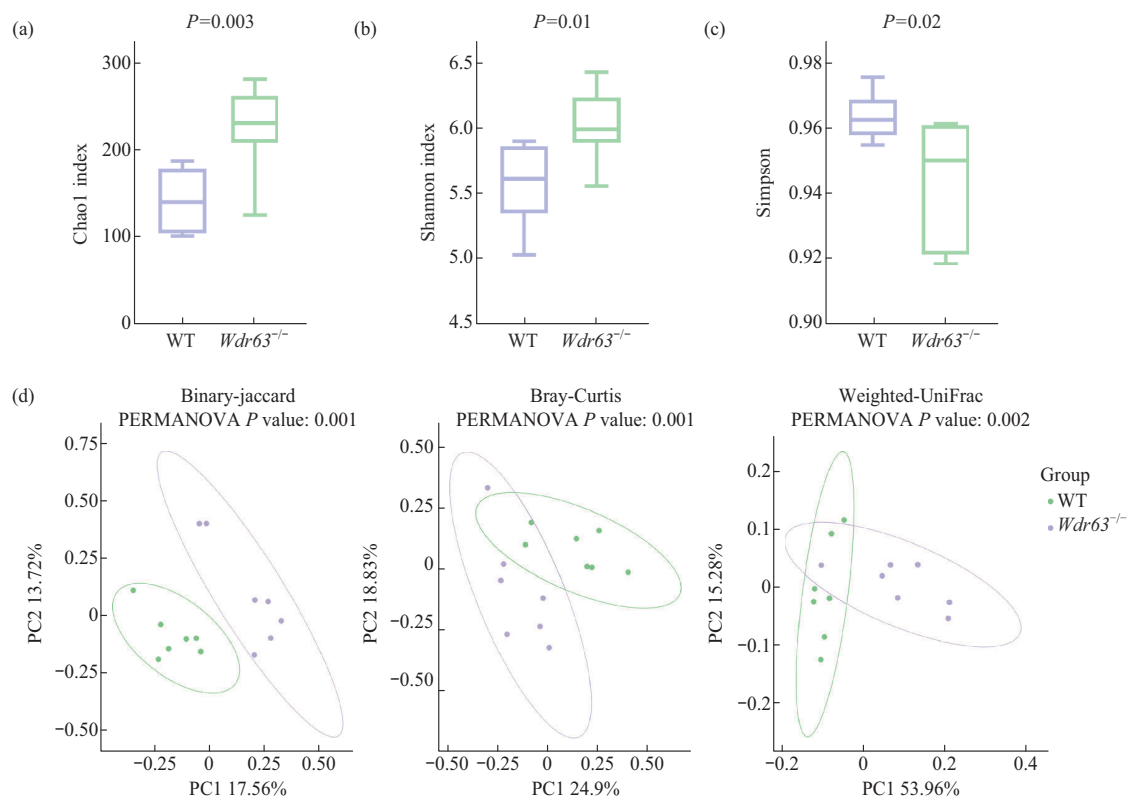


Fig. 4 *Wdr63* deletion affects the abundance and diversity of gut microbiota

(a) Chao1 index. Assess the actual number of species in the community, the larger the value, the higher the richness of the microbial community. (b, c) Shannon index (b) and Simpson index (c) reveal the microbial diversity in the samples; the larger the Shannon index, the greater the microbial diversity, whereas the Simpson index showed the opposite trend. (d) Principal coordinate analysis. Based on the Binary-Jaccard, Bray-Curtis, and Weighted-UniFrac algorithms. $P < 0.05$ was statistically significant.

We analyzed the composition of flora at the phylum and genus levels, studied the impact of WDR63 on the intestinal microbiota's structure. The results showed that at the phylum level, Bacteroidota and Firmicutes were the main occupying flora (Figure 5a). The amount of Bacteroidota was less in *Wdr63*^{-/-} mice (Figure 5b), whereas the amount of Firmicutes (Figure 5c) and Deferribacterota was higher, and the ratio of Firmicutes to Bacteroidota was elevated (Figure 5d). At the genus level, *Muribaculaceae*, *Prevotellaceae*_UCG-001, *Prevotellaceae*_NK3B31_

group, *Lactobacillus*, *Alistipes*, *Parabacteroides*, and *Clostridia*_UCG-014, etc. decreased in abundance in *Wdr63*^{-/-} mice; *Lachnospiraceae*_NK4A136_group, *Helicobacter*, etc. increased in abundance (Figure 5e). LEfSe was used to analyze the differentially abundant microbial between two groups. As the results demonstrate, the main differential species enriched in WT mice were *Bacteroidales* and *Muribaculaceae*, and the main differential species enriched in *Wdr63*^{-/-} mice were *Clostridia* and *Firmicutes* (Figure 5f, g).

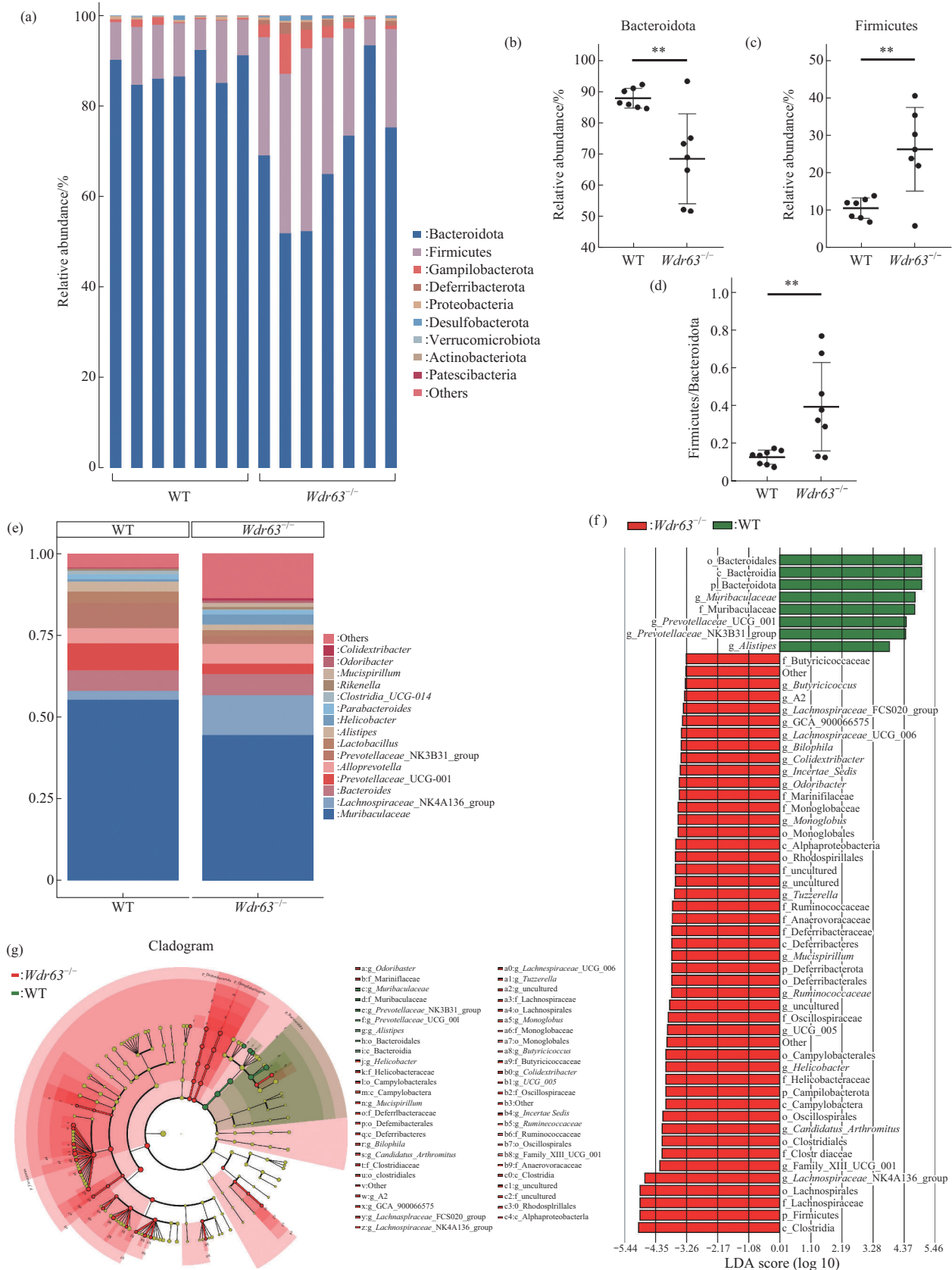


Fig. 5 *Wdr63* deletion affects gut microbiota balance

(a) Relative abundance of bacteria at the phylum level. (b) The percentage of Bacteroidota at the phylum level. (c) The percentage of Firmicutes at the phylum level. (d) The proportion of thick-walled Firmicutes/Bacteroidota at the phylum level. (e) Genus-level relative abundance of bacteria (>5%). (f) Differential species score plot in LEfSe analysis. (g) Annotated branching plots of differential species. The statistical indicators were analyzed using two-tailed unpaired *t* test, with statistical significance being characterized by *P*<0.05. Significance levels: ***P*<0.01.

To understand the role of WDR63 on gut microbiota function, we used PICRUSt to predict functional changes in the gut microbiota based on changes in their abundance. Through functional prediction using the Kyoto Encyclopedia of Genes and Genomes (KEGG) pathway analysis, we found

that several functional metabolic pathways of the microbiota differed significantly between the WT and *Wdr63*^{-/-} mice, including cell motility, bacterial chemotaxis, ansamycin biosynthesis, and biofilm formation-*Pseudomonas aeruginosa* (Figure 6a, b).

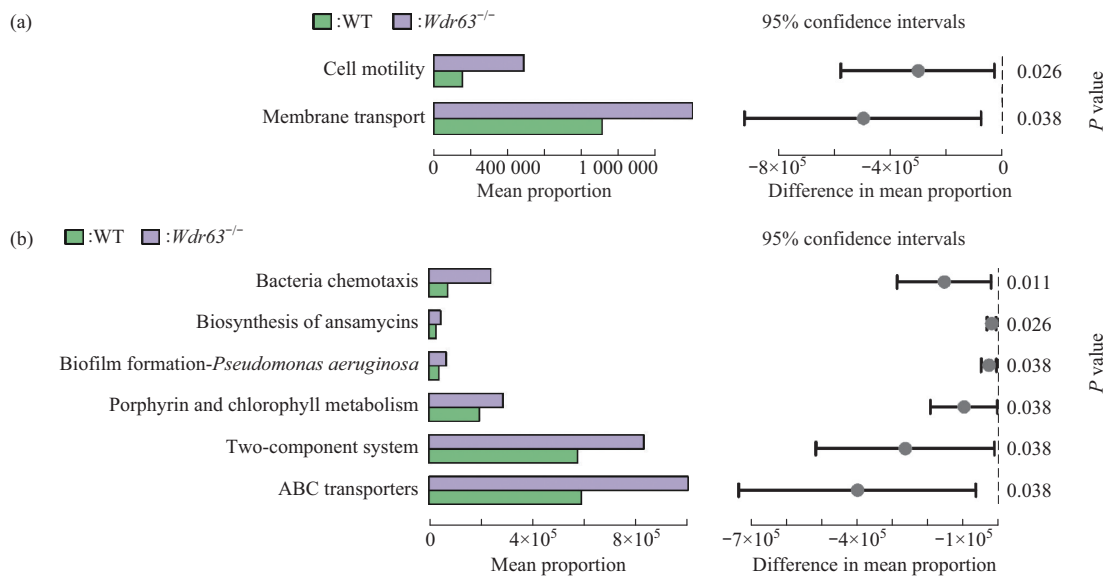


Fig. 6 Effect of *Wdr63* deletion on gut microbiota function

(a) Bar graph of KEGG level 2 difference results, with the average abundance of the pathway in each group on the left bar, and 95% confidence intervals for the comparison of between-group variation and the corresponding significance *P* values on the right. (b) Bar graph of KEGG level 3 difference results.

3 Discussion

The pathogenesis of UC is marked by an imbalance in intestinal immunoreactivity. Aberrant immune responses and imbalances in the gut flora disrupt intestinal homeostasis, leading to an exaggerated inflammatory response^[36]. DSS-induced UC serves as a classic disease model for studying immune homeostasis. We induced colitis using 3% DSS, with observed symptoms such as dilute stools, blood in the stools, body mass loss, shortened colon length, and typical signs of tiny ulcer formation and inflammatory cell infiltration. This indicates successful replication of DSS-induced colitis in mice. Notably, *Wdr63*^{-/-} mice exhibited more severe symptoms of UC, including colonic shortening and body mass loss, compared to WT mice. Histological examination revealed that the degree of colonic injury was more severe in *Wdr63*^{-/-} mice. Researchers found that the Th17/Treg cell balance is essential for

immune homeostasis in the colonic ecosystem^[37-38]. And the dynamic remodeling of the actin cytoskeleton is vital for T lymphocyte effector function^[23]. Because WDR63 is involved in actin cytoskeleton formation, we propose that the exacerbation of colitis resulting from WDR63 deletion may be related to the disruption of the Th17/Treg balance.

Th17 and Treg cells are pivotal components of the adaptive immune response and demonstrate antagonistic effects in immune diseases^[39]. The transcription factors *FOXP3* and *RORγt* that drive Treg and Th17 cells lineage differentiation, respectively, are strictly regulated in different tissue microenvironments. Alterations in the number or nature of Foxp3 Treg cells or RORγt Th17 cells may result in inflammatory diseases in humans^[40]. Our results revealed an increase in Th17 cells and a decrease in Treg cells in the lymph nodes of *Wdr63*^{-/-} mice with colitis compared to WT mice. Additionally, *Wdr63*^{-/-} mice exhibited a significant increase in

ROR γ t Th17 cells and a significant decrease in Foxp3 Treg cells in colonic tissues. Previous studies have highlighted that cytokines control the differentiation of Treg and Th17 cells in inflammatory bowel disease^[41]. Among these, IL-17A is the main pro-inflammatory cytokine produced by Th17 lymphocytes^[42]. Pro-inflammatory Th17 cells secrete huge amounts of IL-17A when activated, leading to colonic mucosal damage^[43]. In contrast, Treg cells exhibit anti-inflammatory effects and promote colonic mucosal repair by secreting IL-10^[44-45]. ELISA results showed a decrease in IL-10 levels and an increase in IL-17A levels in the serum of colitic *Wdr63*^{-/-} mice, further confirming the role of WDR63 in regulating the Th17/Treg balance and maintaining immune homeostasis. Studies show that Notch is a critical regulator of T cell differentiation, and the actin cytoskeleton affects signal transduction between T cells and Notch^[27]. We speculate that WDR63 affects the differentiation of Th17 and Treg cells through the regulation of Notch signaling. Furthermore, WDR63 has been demonstrated as a regulator of cell migration, invasion, and metastasis by inhibiting actin polymerization mediated by the Arp2/3 complex^[34]. So WDR63 may influence Th17/Treg cell homeostasis by acting on Arp2/3 complex. In addition to T cells, other immune cells, including macrophages, neutrophils, and dendritic cells, also play a significant role in the immune response to UC. M1 macrophages are pro-inflammatory and help fight bacteria, while M2 macrophages express high levels of the anti-inflammatory cytokine IL-10, which plays a role in tissue homeostasis, inflammation suppression and tissue repair^[46-47]. We speculate that WDR63 may ameliorate the severity of colitis by enhancing a positive feedback loop between M2 macrophages and Treg cells. However, the specific regulatory mechanism remains to be further investigated.

Gut microbes play a crucial role in regulating immune responses and influencing the progression of IBD. As components of the gut's physical barrier, gut microbiota is associated with maintaining gut health, immune homeostasis, and metabolic homeostasis^[48]. Gut microbiota co-evolves with the host's intestinal environment, and its effects on human health and disease are significant. Targeted modulation of gut microbiota homeostasis is an emerging therapeutic strategy for various diseases^[49]. In our study, we observed increased gut microbial abundance and

diversity in *Wdr63*^{-/-} mice. The structure of gut microbial community showed significant differences between the two groups. The abundance of Bacteroidota decreased in the *Wdr63*^{-/-} group, while the abundance of Firmicutes and Deferribacterota increased. The ratio of Firmicutes/Bacteroidota also increased. Previous studies have shown that Bacteroidetes are beneficial intestinal commensals. They maintain a complex relationship with the host and play a positive role in partial immunomodulation of the immune system^[50]. An elevated Firmicutes/Bacteroidota ratio is considered a marker of ecological dysbiosis, which has previously been demonstrated to be linked to disease development such as obesity^[51], autism spectrum disorders^[52], and non-alcoholic fatty liver disease^[53]. Furthermore, we found that the abundance of *Muribaculaceae*, a differentiated species predominantly enriched in WT mice, was significantly reduced in *Wdr63*^{-/-} mice. *Muribaculaceae* is negatively associated with inflammatory states and can inhibit CD8 T cells activation to tolerate the immune stimulation^[54]. *Muribaculaceae* is known to contribute to the production of short-chain fatty acids, which play a key metabolic role in prolonging lifespan^[55]. Predictive analysis of metabolic pathways revealed variations in functional genes within microbial communities, specifically regarding cell motility and bacterial chemotaxis. Bacterial chemotaxis is a crucial factor in various biological processes, including biofilm development, bacterial pathogens, and host infection^[56]. Our experimental results indicate that WDR63 takes an important part in promoting beneficial intestinal bacteria and regulating the balance of microbial communities.

4 Conclusion

Taken together, our experiments demonstrated that WDR63 maintains Th17/Treg balance *via* down-regulating Th17 cells and up-regulating Treg cells in DSS-induced colitis mice. It also regulates microbial community homeostasis in the gut. These ultimately inhibit inflammatory progression. The study has elucidated the key genes involved in inhibiting the progression of colitis, and suggested the mechanism that may be related to the regulation of immune homeostasis of Th17/Treg cells. These findings provide a theoretical basis and candidate targets for

the study and treatment of immune-inflammatory diseases such as colitis.

Supplementary Available online (<http://www.pibb.ac.cn>, <http://www.cnki.net>): PIBB_20240148_Figure_S1.pdf

References

- [1] Dai C, Huang YH, Jiang M. Combination therapy in inflammatory bowel disease: current evidence and perspectives. *Int Immunopharmacol*, 2023, **114**: 109545
- [2] Ye Z, Yang X, Deng B, *et al.* Prevention of DSS-induced colitis in mice with water kefir microbiota *via* anti-inflammatory and microbiota-balancing activity. *Food Funct*, 2023, **14**(15): 6813-6827
- [3] Ng S C, Shi H Y, Hamidi N, *et al.* Worldwide incidence and prevalence of inflammatory bowel disease in the 21st century: a systematic review of population-based studies. *Lancet*, 2017, **390**(10114): 2769-2778
- [4] GBD 2017 Inflammatory Bowel Disease Collaborators. The global, regional, and national burden of inflammatory bowel disease in 195 countries and territories, 1990-2017: a systematic analysis for the Global Burden of Disease Study 2017. *Lancet Gastroenterol Hepatol*, 2020, **5**(1): 17-30
- [5] Agrawal M, Allin K H, Petralia F, *et al.* Multiomics to elucidate inflammatory bowel disease risk factors and pathways. *Nat Rev Gastroenterol Hepatol*, 2022, **19**(6): 399-409
- [6] Korta A, Kula J, Gomułka K. The role of IL-23 in the pathogenesis and therapy of inflammatory bowel disease. *Int J Mol Sci*, 2023, **24**(12): 10172
- [7] Sartor R B, Wu G D. Roles for intestinal bacteria, viruses, and fungi in pathogenesis of inflammatory bowel diseases and therapeutic approaches. *Gastroenterology*, 2017, **152**(2): 327-339.e4
- [8] Zhao J, Lu Q, Liu Y, *et al.* Th17 cells in inflammatory bowel disease: cytokines, plasticity, and therapies. *J Immunol Res*, 2021, **2021**: 8816041
- [9] Zhang S, Cao Y, Huang Y, *et al.* Aqueous *M. oleifera* leaf extract alleviates DSS-induced colitis in mice through suppression of inflammation. *J Ethnopharmacol*, 2024, **318**(Pt B): 116929
- [10] Wang L, Zhang H, Tang F, *et al.* Therapeutic effects of *Valeriana jatamansi* on ulcerative colitis: insights into mechanisms of action through metabolomics and microbiome analysis. *J Proteome Res*, 2023, **22**(8): 2669-2682
- [11] Ruterbusch M, Pruner K B, Shehata L, *et al.* *In vivo* CD4⁺ T cell differentiation and function: revisiting the Th1/Th2 paradigm. *Annu Rev Immunol*, 2020, **38**: 705-725
- [12] Knochelmann H M, Dwyer C J, Bailey S R, *et al.* When worlds collide: Th17 and Treg cells in cancer and autoimmunity. *Cell Mol Immunol*, 2018, **15**(5): 458-469
- [13] Kajdaniuk D, Foltyn W, Morawiec-Szymonik E, *et al.* Th17 cytokines and factors modulating their activity in patients with pernicious anemia. *Immunol Res*, 2023, **71**(6): 873-882
- [14] Littman D R, Rudensky A Y. Th17 and regulatory T cells in mediating and restraining inflammation. *Cell*, 2010, **140**(6): 845-858
- [15] Dominguez-Villar M, Hafler D A. Regulatory T cells in autoimmune disease. *Nat Immunol*, 2018, **19**(7): 665-673
- [16] Wang S, Ruan P, Peng L, *et al.* Cytokine-stimulated human amniotic epithelial cells alleviate DSS-induced colitis in mice through anti-inflammation and regulating Th17/Treg balance. *Int Immunopharmacol*, 2023, **120**: 110265
- [17] Gao R, Zhang W, Jiang Y, *et al.* Eldecalcitol effectively prevents alveolar bone loss by partially improving Th17/Treg cell balance in diabetes-associated periodontitis. *Front Bioeng Biotechnol*, 2023, **11**: 1070117
- [18] Zhao X, Yi Y, Jiang C, *et al.* Gancao Fuzi decoction regulates the Th17/Treg cell imbalance in rheumatoid arthritis by targeting *Foxp3 via miR-34a*. *J Ethnopharmacol*, 2023, **301**: 115837
- [19] Zou M Y, Wang Y J, Liu Y, *et al.* Huangshan floral mushroom polysaccharide ameliorates dextran sulfate sodium-induced colitis in mice by modulating Th17/treg balance in a gut microbiota-dependent manner. *Mol Nutr Food Res*, 2023, **67**(2): e2200408
- [20] Lee G R. The balance of Th17 versus Treg cells in autoimmunity. *Int J Mol Sci*, 2018, **19**(3): 730
- [21] Garcia G, Homentcovschi S, Kelet N, *et al.* Imaging of actin cytoskeletal integrity during aging in *C. elegans*. *Methods Mol Biol*, 2022, **2364**: 101-137
- [22] Lian G, Sheen V L. Cytoskeletal proteins in cortical development and disease: actin associated proteins in periventricular heterotopia. *Front Cell Neurosci*, 2015, **9**: 99
- [23] Reicher B, Barda-Saad M. Multiple pathways leading from the T-cell antigen receptor to the actin cytoskeleton network. *FEBS Lett*, 2010, **584**(24): 4858-4864
- [24] Fritzsche M, Fernandes R A, Chang V T, *et al.* Cytoskeletal actin dynamics shape a ramifying actin network underpinning immunological synapse formation. *Sci Adv*, 2017, **3**(6): e1603032
- [25] Sadhu L, Tsopoulidis N, Hasanuzzaman M, *et al.* ARPC5 isoforms and their regulation by calcium-calmodulin-N-WASP drive distinct Arp2/3-dependent actin remodeling events in CD4 T cells. *eLife*, 2023, **12**: e82450
- [26] Thompson S B, Waldman M M, Jacobelli J. Polymerization power: effectors of actin polymerization as regulators of T lymphocyte migration through complex environments. *FEBS J*, 2022, **289**(20): 6154-6171
- [27] Britton G J, Ambler R, Clark D J, *et al.* PKC θ links proximal T cell and Notch signaling through localized regulation of the actin cytoskeleton. *Elife*, 2017, **6**: e20003
- [28] Dohnke S, Moehser S, Surnov A, *et al.* Role of dynamic actin cytoskeleton remodeling in *Foxp3*⁺ regulatory TCell development and function: implications for osteoclastogenesis. *Front Immunol*, 2022, **13**: 836646
- [29] Diao S, Yang D M, Dong R, *et al.* Enriched trimethylation of lysine 4 of histone H3 of WDR63 enhanced osteogenic differentiation potentials of stem cells from apical papilla. *J Endod*, 2015, **41**(2): 205-211
- [30] Hofmeister W, Pettersson M, Kurtoglu D, *et al.* Targeted copy

- number screening highlights an intragenic deletion of WDR63 as the likely cause of human occipital encephalocele and abnormal CNS development in zebrafish. *Hum Mutat*, 2018, **39**(4): 495-505
- [31] Lu S, Gu Y, Wu Y, *et al.* Bi-allelic variants in human WDR63 cause male infertility *via* abnormal inner dynein arms assembly. *Cell Discov*, 2021, **7**(1): 110
- [32] Zhang Y, Chen Y, Zheng J, *et al.* Vertebrate Dynein-f depends on Wdr78 for axonemal localization and is essential for ciliary beat. *J Mol Cell Biol*, 2019, **11**(5): 383-394
- [33] Young S A M, Miyata H, Satouh Y, *et al.* CRISPR/Cas9-mediated rapid generation of multiple mouse lines identified Ccdc63 as essential for spermiogenesis. *Int J Mol Sci*, 2015, **16**(10): 24732-24750
- [34] Zhao K, Wang D, Zhao X, *et al.* WDR63 inhibits Arp2/3-dependent actin polymerization and mediates the function of p53 in suppressing metastasis. *EMBO Rep*, 2020, **21**(4): e49269
- [35] Rachmilewitz D, Stamler J S, Karmeli F, *et al.* Peroxynitrite-induced rat colitis--a new model of colonic inflammation. *Gastroenterology*, 1993, **105**(6): 1681-1688
- [36] Bao M, Wang K, Li J, *et al.* ROS Scavenging and inflammation-directed polydopamine nanoparticles regulate gut immunity and flora therapy in inflammatory bowel disease. *Acta Biomater*, 2023, **161**: 250-264
- [37] Eastaff-Leung N, Mabarrack N, Barbour A, *et al.* Foxp3+ regulatory T cells, Th17 effector cells, and cytokine environment in inflammatory bowel disease. *J Clin Immunol*, 2010, **30**(1): 80-89
- [38] Yan J B, Luo M M, Chen Z Y, *et al.* The function and role of the Th17/Treg cell balance in inflammatory bowel disease. *J Immunol Res*, 2020, **2020**: 8813558
- [39] Zhang S, Gang X, Yang S, *et al.* The alterations in and the role of the Th17/Treg balance in metabolic diseases. *Front Immunol*, 2021, **12**: 678355
- [40] Zhang W, Liu X, Zhu Y, *et al.* Transcriptional and posttranslational regulation of Th17/Treg balance in health and disease. *Eur J Immunol*, 2021, **51**(9): 2137-2150
- [41] Sanchez-Munoz F, Dominguez-Lopez A, Yamamoto-Furusho J K. Role of cytokines in inflammatory bowel disease. *World J Gastroenterol*, 2008, **14**(27): 4280-4288
- [42] Abraham C, Cho J. Interleukin-23/Th17 pathways and inflammatory bowel disease. *Inflamm Bowel Dis*, 2009, **15**(7): 1090-1100
- [43] Owaga E, Hsieh R H, Mugendi B, *et al.* Th17 cells as potential probiotic therapeutic targets in inflammatory bowel diseases. *Int J Mol Sci*, 2015, **16**(9): 20841-20858
- [44] Sarabayrouse G, Alameddine J, Altare F, *et al.* Microbiota-specific CD4CD8 $\alpha\alpha$ tregs: role in intestinal immune homeostasis and implications for IBD. *Front Immunol*, 2015, **6**: 522
- [45] Chang Y, Zhai L, Peng J, *et al.* Phytochemicals as regulators of Th17/Treg balance in inflammatory bowel diseases. *Biomedicine Pharmacother*, 2021, **141**: 111931
- [46] Nguyen Q P, Deng T Z, Witherden D A, *et al.* Origins of CD4⁺ circulating and tissue-resident memory T-cells. *Immunology*, 2019, **157**(1): 3-12
- [47] Deli F, Romano F, Gualini G, *et al.* Resident memory T cells: possible players in periodontal disease recurrence. *J Periodontal Res*, 2020, **55**(2): 324-330
- [48] Xiao Q P, Zhong Y B, Kang Z P, *et al.* Curcumin regulates the homeostasis of Th17/Treg and improves the composition of gut microbiota in type 2 diabetic mice with colitis. *Phytother Res*, 2022, **36**(4): 1708-1723
- [49] Kayama H, Okumura R, Takeda K. Interaction between the microbiota, epithelia, and immune cells in the intestine. *Annu Rev Immunol*, 2020, **38**: 23-48
- [50] Wexler H M. *Bacteroides*: the good, the bad, and the nitty-gritty. *Clin Microbiol Rev*, 2007, **20**(4): 593-621
- [51] Koliada A, Syzenko G, Moseiko V, *et al.* Association between body mass index and *Firmicutes/Bacteroidetes* ratio in an adult Ukrainian population. *BMC Microbiol*, 2017, **17**(1): 120
- [52] Strati F, Cavalieri D, Albanese D, *et al.* New evidences on the altered gut microbiota in autism spectrum disorders. *Microbiome*, 2017, **5**(1): 24
- [53] Fernández-Musoles R, García Tejedor A, Laparra J M. Immunonutritional contribution of gut microbiota to fatty liver disease. *Nutr Hosp*, 2020, **37**(1): 193-206
- [54] Hao H, Zhang X, Tong L, *et al.* Effect of extracellular vesicles derived from *Lactobacillus plantarum* Q7 on gut microbiota and ulcerative colitis in mice. *Front Immunol*, 2021, **12**: 777147
- [55] Ratto D, Roda E, Romeo M, *et al.* The many ages of microbiome-gut-brain axis. *Nutrients*, 2022, **14**(14): 2937
- [56] Karmakar R. State of the art of bacterial chemotaxis. *J Basic Microbiol*, 2021, **61**(5): 366-379

Wdr63缺失可能通过影响Th17/Treg平衡和肠道菌群来加重溃疡性结肠炎*

朱豪¹⁾ 朱梦远¹⁾ 曹杨杨¹⁾ 杨秋波^{1)**} 范志朋^{1,2,3)**}

¹⁾ 首都医科大学附属北京口腔医院, 北京口腔医学研究所, 北京 100050;

²⁾ 首都医科大学口腔健康北京实验室, 北京 100069; ³⁾ 中国医学科学院, 牙发育与再生创新单元, 北京 100069)

摘要 目的 溃疡性结肠炎是一种常见的免疫炎症性疾病, Th17/Treg细胞失衡和肠道微生物群失调在其发病机制中起主要作用。肌动蛋白细胞骨架有助于调节Th17和Treg细胞的增殖、分化和迁移。Wdr63是一种含WD重复结构域的基因, 与肌动蛋白细胞骨架的形成和功能调控密切相关。近来研究表明, WDR63可能通过抑制肌动蛋白聚合作为细胞迁移的调节因子。本文拟探究WDR63对Th17/Treg细胞的调节作用及对溃疡性结肠炎的影响。**方法** 本文构建Wdr63^{-/-}小鼠, 使用葡聚糖硫酸钠盐诱导小鼠结肠炎, 收集结肠组织进行组织病理学染色, 收集肠系膜淋巴结进行流式细胞术分析, 收集健康小鼠粪便进行微生物多样性检测。**结果** 与野生型结肠炎小鼠相比, Wdr63^{-/-}结肠炎小鼠的结肠组织缩短更明显, 疾病活动指数和组织学损伤指数评分更高, 结肠组织和肠系膜淋巴结中的Treg细胞减少, Th17细胞增多, 抗炎细胞因子IL-10水平较低, 而促炎细胞因子IL-17A水平较高。此外, WDR63在维持肠道微生物群稳态方面显示出积极作用, 它能够维持拟杆菌门和厚壁菌门的平衡, 促进与免疫炎症相关的肠道有益菌的形成。**结论** Wdr63缺失加剧了小鼠溃疡性结肠炎, WDR63可能通过调节Th17/Treg平衡和维持肠道微生物群稳态来抑制结肠炎症。

关键词 Wdr63, Th17/Treg, 溃疡性结肠炎, 炎症, 免疫, 微生物

中图分类号 R392.1

DOI: 10.16476/j.pibb.2024.0148

CSTR: 32369.14.pibb.20240148

* 国家自然科学基金(82130028), 国家重点研发计划(2022YFA1104401), 中国医学科学院医学创新基金(2019-I2M-5-031)和首都医科大学北京口腔医院创新研究项目(CXTD202204)资助。

** 通讯联系人。

范志朋 Tel: 010-57099311, E-mail: zpfan@ccmu.edu.cn

杨秋波 Tel: 010-57099319, E-mail: qiuboyang2003@163.com

收稿日期: 2024-04-08, 接受日期: 2024-08-21